Progress In Electromagnetics Research M, Vol. 10, 25–38, 2009

COMPARATIVE ANALYSIS OF SPLIT-RING RESONATORS FOR TUNABLE NEGATIVE PERMEABILITY METAMATERIALS BASED ON ANISOTROPIC DIELECTRIC SUBSTRATES

J.-Y. Chen

Center for General Education
Hsing Kuo University of Management
No. 600, Sec. 3, Taijing Blvd., Annan District
Tainan 709, Taiwan, R.O.C.

W.-L. Chen

Institute of Manufacturing Engineering
National Cheng Kung University
No. 1, University Road, Tainan City 701, Taiwan, R.O.C.

J.-Y. Yeh

Department of Management Information Science
Chung Hwa University of Medical Technology
No. 89, Wen-Hwa 1st ST. Jen-Te Hsiang
Tainan Hsien 717, Taiwan, R.O.C.

L.-W. Chen

Department of Mechanical Engineering
National Cheng Kung University
No. 1, University Road, Tainan City 701, Taiwan, R.O.C.

C.-C. Wang

Institute of Manufacturing Engineering
National Cheng Kung University
No. 1, University Road, Tainan City 701, Taiwan, R.O.C.

Corresponding author: C.-C. Wang (ccwang@mail.ncku.edu.tw).

Abstract—The magnetic resonance of various split ring resonators (SRRs) is numerically investigated to analyze the dependence of the resonance frequency on their parameter designs. The behavior of the magnetic resonance frequency in the configuration of the 2-cut single-ring SRR (2C-SRR) shows a larger shift in relation to the changes of the SRR size scaling, split width and substrate permittivity. A new magnetic particle formed by the 2C-SRR structure incorporating nematic liquid crystals (LCs) into the multilayered substrate is proposed for the realization of a tunable magnetic metamaterial. When using such inclusions, the tuning range of the magnetic resonance conditions could be as wide as ~ 1.1 GHz via changing the orientation of LC molecules by 90°.

1. INTRODUCTION

In many experiments and simulations, it has been proposed that artificially constructed materials may have unavailable properties in natural materials [1]. Among such composite materials, split ring resonators (SRRs) have received growing concern in recent years [2, 3]. In the long wavelength limit, composite structured materials consisting of periodic or random scattering elements could response to the incident electromagnetic radiation as continuous materials, so that the effective medium theory is applicable. By placing the SRRs/wires along the two orthogonal axes in a lattice, Shelby et al. have realized left-handed metamaterials (LHMs) with simultaneous negative permeability and permittivity [4]. Therefore, SRRs/wire arrays can be considered as a generic electromagnetic metamaterial, in which the SRRs play an important role for the property of negative permeability in LHMs with negative refractive index.

Basically, the narrow frequency band of negative permeability is essentially determined by the magnetic resonance frequency of SRR structures, whereas a broad frequency window of negative permittivity is shown in wire arrays. The domination of developing LHMs is the realization of the negative permeability. Even if other structures such as Ω-, S-, and L-shaped resonators were proposed [5–7], the left-handed passband frequency in most of these cases is relatively narrow. All the interesting effects realized by metamaterials, such as negative refraction, perfect lensing [8], cloaking [9], filtration [10], and antennas [11], are confined to a fixed narrow spectral bandwidth. Thus, it is highly desirable that the operating frequency of metamaterials could be tuned so as to relieve these limitations.

As the potential applications offered by passive composites are already numerous and still developing, there have been some efforts

to examine how to dynamically tune or adjust the electromagnetic properties of metamaterials. In essence, a SRR can be considered as a small LC circuit composed of an inductance L and a capacitance C. The electromagnetic response of SRRs excited by a time-varying magnetic field parallel to the ring axis results from a resonant exchange of energy between the electrostatic fields in the capacitive gaps (splits) and the inductive currents in the rings. Hence, it is possible to achieve the manipulation over the structure via altering the resonance conditions. For example, simulations and experiments performed at microwave frequencies have shown that metamaterials can be controlled by mounting varactors or photocapacitances to their inner structures [12–15]. In [3], the authors proposed a tunable LHM based on the broadside-coupled SRR (BC-SRR). The magnetic resonance frequency can be controlled by the relative slip of the substrates. Different from adjusting the equivalent capacitance of SRRs, the tunable left-handed transmission properties can be realized by the mechanism of magnetically tuning the inductance via introducing yttrium iron garnet rods into SRRs/wire arrays [16]. In particular, liquid crystals (LCs) stand out as the preferred means of achieving tunability due to their feature of very large dielectric anisotropy sensitive to external fields. By means of tuning the director orientation of the infiltrated anisotropic LCs, the magnetic resonance can be controlled to achieve the reconfiguration of the negative index or permeability metamaterials [17–19]. In brief, tunability is introduced by ensuring that the attached components are made of variable capacitance diodes, photocapacitance, mechanical tuners, ferrites, LCs, etc.

In this paper, we compare some known geometries of SRR structures [2, 11–15, 19, 20] in order to further maximize the tuning effect of artificial magnetism. A new tunable negative permeability metamaterial, which is composed of a periodic array of SRRs and sandwich substrates infiltrated with nematic LCs, will be demonstrated. The dependence of the resonance frequency for various SRRs on the factors, such as the ring diameter, radial and azimuthal gap, electric permittivity and the thickness of the substrate, and the director orientation of the embedding LCs, will be investigated. It can be seen that the magnetic resonance frequency is very sensitive to the variation of the electromagnetic properties of the substrate, especially for the geometry of the 2-cut single-ring SRR (2C-SRR). By using an external field excitation on the alignment of LCs, the 2C-SRR structure provides a good tunability on the frequency shift of the magnetic resonant response.

2. SIMULATION MODELS OF SRRS

This section will describe the models for the composite negative magnetic permeability media. Four types of SRRs from which the various resonators are constructed are shown in Fig. 1. The basic unit cells are composed of a 1-cut single ring SRR (1C-SRR), a 2C-SRR, an edge-coupled SRR (EC-SRR), and a BC-SRR, respectively. Using a shadow mask/etching technique, printed circuit boards with SRRs can be fabricated on one or two sides. The original dimensions of the four SRR structures are indicated in the caption of Fig. 1. d is the width of the split. All rings and substrates of the four SRRs have the same heights and thicknesses. The direction of electromagnetic wave propagation and electric field are parallel to the SRR plane. The SRR resonance is excited by a time-varying magnetic field parallel to the ring axis.

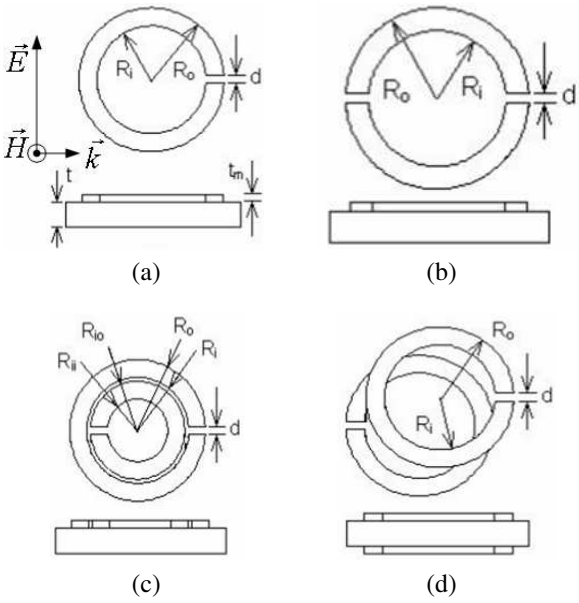

Figure 1. The split ring resonators (SRRs): (a) 1-cut single ring SRR (1C-SRR); (b) 2-cut single ring SRR (2C-SRR); (c) edge-coupled SRR (EC-SRR); (d) broadside-coupled SRR (BC-SRR). The dimensions chosen for numerical calculations are $R_i = 2.7\,\text{mm}$, $R_o = 3.6\,\text{mm}$, $R_{io} = 2.5\,\text{mm}$, $R_{ii} = 1.6\,\text{mm}$, $t = 0.25\,\text{mm}$, and $t_m = 0.017\,\text{mm}$ under the scale factor $sf = 1$. The relative permittivity and the dielectric loss tangent of the substrate are 3.8 and 0.02, respectively.

In order to obtain the resonance characteristics in the SRR structures, electromagnetic simulations are performed by using the commercial software Ansoft HFSS, which is a three-dimensional full-wave solver employing the finite element method (FEM). For the determination of the resonance frequencies of the structures under consideration, the SRR cell shown in Fig. 2 is included along the propagation direction. The outer box is the simulation space, and the size of which is $8\times8\times24\,\mathrm{mm}^3$. The relative permittivity of the substrate is 3.8, and the relative permeability is 1. Besides, the dielectric loss tangent is fixed to be 0.02. The structures are subjected to an incident plane wave along the y axis from left to right. The E and H fields are polarized along the x and z axes, respectively. Absorption boundary conditions are employed along the propagation direction to limit the calculation region. Periodic boundary conditions are used along the directions that are perpendicular to the propagation direction. For the microwave frequency, the rings are assumed to be made of perfect electrical conductors so that the salient features of transmittance might be visualized. In addition, this option is often used in the simulations of the commercial software. The transmission spectrum can be extracted from the S-parameter calculation. The complex magnetic permeability μ_{eff} of an equivalent metamaterial with respect to the SRR system can also be retrieved from the S-parameters [21]:

$$\mu_{eff} = NZ, \tag{1}$$

where

$$N = \cos^{-1}\left(\left(1 - S_{11}^2 + S_{21}^2\right)/2S_{21}\right)/k\delta, \tag{2}$$

and

$$Z = \sqrt{[(1+S_{11})^2 - S_{21}^2]/\ [(1-S_{11})^2 - S_{21}^2]}. \tag{3}$$

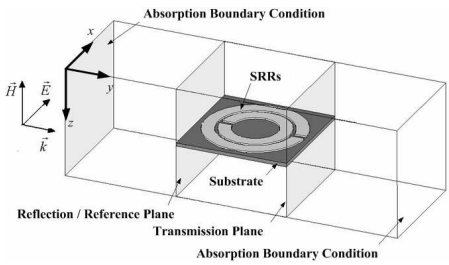

Figure 2. Schematic of the basic unit cell for simulations. The periodic boundary conditions are in the x and z directions. The outer box size is $8 \times 8 \times 24\,\mathrm{mm}^3$.

Here, S_{11} and S_{21} are the reflection and transmission coefficients of the S-parameters, respectively. k is the incident wavenumber. When characterizing the SRR system to be used as an equivalent homogeneous slab, δ is the thickness of such a slab. N and Z are the equivalent refractive index and wave impedance of the slab, respectively.

3. COMPARISON OF CHARACTERISTICS OF SRRS

In order to achieve the case with the maximum variation of artificial magnetism, the elements in Fig. 1 were compared with changed geometric dimensions. The theoretical results for the resonance frequencies were obtained from the transmission spectra of the four SRR structures. The various sets of parameters applied to compare the tuning effect were studied through electromagnetic simulations using the FEM tool. A scaled set of SRR dimensions is based on the scale factor sf given by

$$sf = P_{current}/P_{original}, \tag{4}$$

where $P_{original}$ represents the parameters of the original structure for the dimensions of R_i, R_o, R_{io}, and R_{ii} listed in the caption of Fig. 1. $P_{current}$ describes the parameters of the scaled structure. As seen from

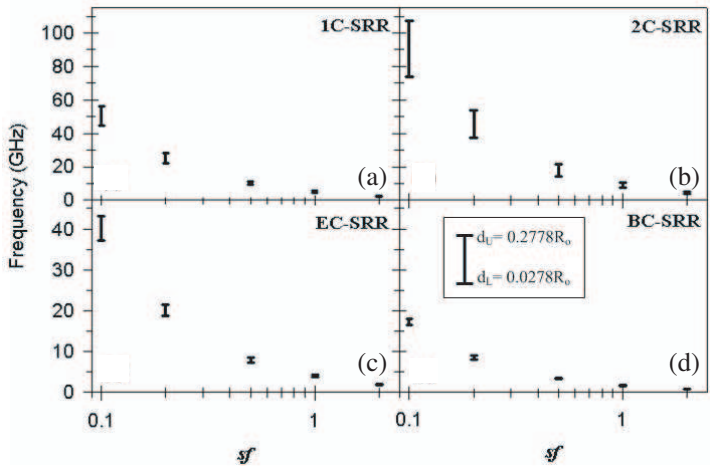

Figure 3. Dependence of the magnetic resonance frequency on the scalar factor sf for the four kinds of SRRs: (a) 1C-SRR; (b) 2C-SRR; (c) EC-SRR; (d) BC-SRR. Error bars indicate the variation of the width d of the split between the upper limit d_U and the lower limit d_L.

Fig. 3, it is shown that the scaled down sets of dimensions for all types of SRRs yield the blue-shift effect of the magnetic resonance frequency. Under different split widths (from the lower limit d_L to the upper limit d_U), simulation results show that increasing the split widths increases the resonance frequency of the SRR structure. It is known that SRRs can be modeled as LC resonant tanks, with its resonance frequency ($\omega_m = 1/\sqrt{L_{eff}C_{eff}}$) determined by the effective inductance L_{eff} from the metal rings and effective capacitance C_{eff} through the splits in the rings or the gaps between the rings. The capacitance scales proportionally to SRR size, provided that all SRR dimensions are scaled down simultaneously. However, the split capacitance scales inversely with the width of the split, and the equivalent capacitance can be reduced by introducing further splits into the ring [22]. As shown in Figs. 3(a) and (b), the resonance frequency increases with the number of cuts in the SRR. In particular, the magnetic response of the SRRs is dominated by the split capacitance [14]. It should be clear that the magnetic resonance frequency could be further increased by reducing the net capacitance, especially for the model of the 2C-SRR structure.

The electromagnetic properties of the substrate on which the SRR is mounted can greatly affect the effective properties of the metamaterials. Fig. 4 shows the dependence of the resonance frequency on the substrate permittivity through examining the transmission minimum. The thickness and the dielectric loss tangent of the substrate are set at $t = 0.25\,\text{mm}$ and 0.02, respectively. It can

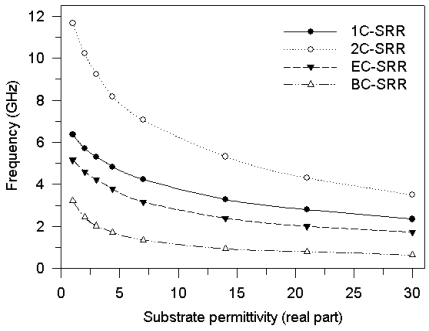

Figure 4. Dependence of the magnetic resonance frequency on the real part of the substrate permittivity for the four kinds of SRRs ($d = 0.2\,\text{mm}$).

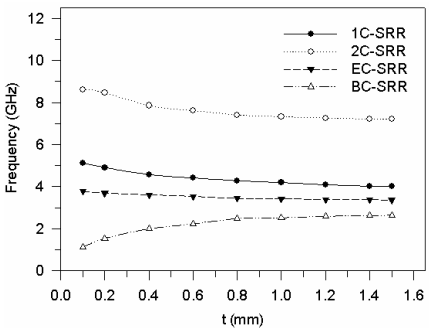

Figure 5. Dependence of the magnetic resonance frequency on the substrate thickness for the four kinds of SRRs ($d = 0.2\,\text{mm}$).

be seen that the resonance frequencies vary significantly with the dielectric property of the substrate, especially for the case of the 2C-SRR structure, in which the frequency drops from $\sim$ 11.65 to $\sim$ 3.49 GHz (the real part of the relative permittivity changes from 1 to 30). The resonance frequency can be lowered by increasing the dielectric constant of the substrate and thus, can be tuned by varying the dielectric properties of the substrate.

The thickness of the substrate is also changed to investigate the effect on the magnetic resonance frequency. The relative permittivity of the substrate is set at 3.8. The response of the resonance frequency varying with the substrate thickness is shown in Fig. 5. Except the case of the BC-SRR structure, the resonance frequency drops as the substrate thickness increases. For the BC-SRR structure, raising the substrate thickness decreases the effective capacitance between the rings so that the resonance frequency increases with the thickness. It is also noticed that the resonance frequencies become saturated as the substrate thickness is beyond 1.0 mm for all the cases. The field caused by the distributed capacitors is confined in the limited small regions even though the substrate thickness increases, so the variation of the effective capacitance becomes less and trends to saturate.

4. RESULTS OF TUNABLE SRRS RELATED TO ANISOTROPIC DIELECTRIC SUBSTRATES

From the standpoint of the metamaterial design, the most important factor characterizing the SRRs is approximately the magnetic resonance frequency. The 2C-SRR structure analyzed in Figs. 3(b) and 4 seems to have the feasibility of designing SRRs with a wide tuning range of negative permeability at resonance. Fig. 6 shows the schematic of the basic unit of the tunable metamaterial, which consists of 2C-SRR patterns printed on the surface of the sandwich glass slabs with infiltration of LC compounds in between. Such a design compared with other configurations [18, 19] can reduce the usage of LCs and relax the cost. The director of the anisotropic LC molecules lies in the x-z plane. A director $\mathbf{n}$ can take any values $\mathbf{n} = \{\sin\theta, 0, \cos\theta\}$ by applying a magnetic or an electric field based on the Fréedericksz effect [23, 24], where θ denotes the rotation angle of the molecular director with respect to the z axis. The thickness of the glass layers and the width of the splits are $h = 0.1$ mm and $d = 0.4$ mm, respectively. The other geometric parameters are the same as the dimensions listed in the caption of Fig. 1. To enlarge the tuning range, advanced nematic LC mixtures doped with tiny ferroelectric particles have been proposed, and their electromagnetic properties can

reveal much higher dielectric anisotropy [25]. In the following analysis on this basis, $\varepsilon_{||} = 17$ and $\varepsilon_{\perp} = 4$ were taken to describe the LC medium, where $\varepsilon_{||}$ and $\varepsilon_{\perp}$ are the relative permittivities for the incident beam polarized parallel and perpendicular to the director axis **n**, respectively. In the infrared and microwave regions, the dielectric and scattering losses in LCs can be neglected, provided that appropriate LC molecules are chosen [23, 24]. It is assumed that the voids infiltrated with LCs are untreated on the surface. When the external field is not applied, the LC becomes isotropic, and its average dielectric constant is $\varepsilon_{av} = (2\varepsilon_{\perp} + \varepsilon_{||})/3$. By means of the identical simulation model shown in Fig. 2, a full wave analysis using the FEM was carried out to determine the transmission property and the tunability of highly anisotropic metamaterials incorporating LCs.

In Fig. 7, the resonance frequencies are provided for the two cases, the LC director along the z axis ($\theta = 0°$, $\varepsilon_z = \varepsilon_{||}$, $\varepsilon_x = \varepsilon_y = \varepsilon_{\perp}$) and the x axis ($\theta = 90°$, $\varepsilon_y = \varepsilon_z = \varepsilon_{\perp}$, $\varepsilon_x = \varepsilon_{||}$), and different thicknesses of the LC layer vary from 0.1 to 1.5 mm. Application of an external field will orient the LC molecules along the field direction. It should be pointed out that not only the split capacitance has the contribution to the total capacitance of the SRR system, but also the variation of the fringe capacitance near the split will greatly affect the effective capacitance of the system [18]. For a specified thickness of the LC layer, as the LC directors are oriented from $\theta = 0°$ to $\theta = 90°$, the change of ε_x from $\varepsilon_{\perp}$ to $\varepsilon_{||}$ increases the fringe capacitance as shown

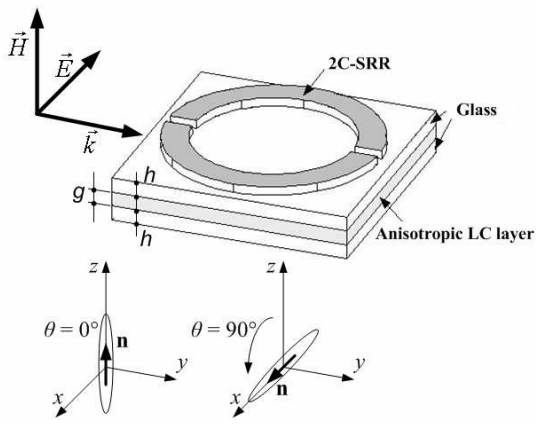

Figure 6. Schematic of the unit cell of the tunable negative permeability metamaterial composed of a 2C-SRR, glass slabs, and LCs. The director of the LC molecule lies in the x-z plane.

in the inset of Fig. 7. Thus, the increase of the capacitance gives rise to the red-shift of the resonance of 2C-SRRs. It is also noticed that the resonance frequencies with respect to the increase of the LC layer thickness become saturated and are similar to the results of Fig. 5. The saturation reveals that the influence of the fringe capacitance is limited to a small region near the split. Besides, the LC layer thickness of $g = 0.3$ mm could provide a larger range for the tuning purpose.

Based on the optimal thickness with the maximum tuning range, Fig. 8 shows the simulated S-parameters, resonance frequencies, and the retrieved effective permeability of the 2C-SRRs for different LC orientations. The resonance dips in the transmission spectra are caused by the intrinsic resonance of SRRs. For the LC influence on magnetic resonance, the tunable metamaterial exhibits negative permeability values in the frequency band ranging from ~ 8.94 GHz to ~ 9.12 GHz for the case of $\theta = 0°$. By increasing the director angle to $\theta = 90°$, a clear red-shift of the frequency band with negative permeability down to 7.85–7.98 GHz can be observed. As shown in the inset of Fig. 8(a), the magnetic resonance frequency is gradually decreased with the LC director angle. In contrast, the real part of the effective permeability at the corresponding resonance frequency shifts toward higher values as the LC director angle is increased from 0° to 90°, as depicted in the inset of Fig. 8(b). The tuning range depends on the control of the dielectric permittivity difference in nematic LC mixtures and LC layer thickness.

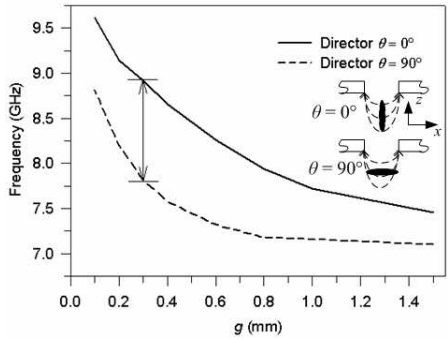

Figure 7. Dependence of the magnetic resonance frequency on the thickness g of the nematic LC layer with respect to the different molecule orientations at $\theta = 0°$ and 90°. The insets show the fringe capacitance effect in relation to the LC molecules and the fringe electric field near the split.

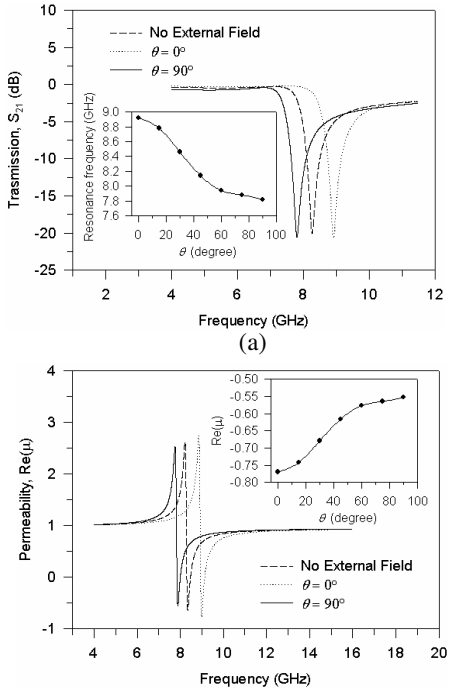

Figure 8. (a) Transmission through arrays of 2C-SRRs under different LC orientations. The inset shows the magnetic resonance frequency as a function of the reorientation angle of the LC molecules. (b) The corresponding effective permeability obtained by the retrieval methods. The inset shows the effective permeability at the magnetic resonance frequency as a function of the rotating angle of the LC director. ($g = 0.3\,\mathrm{mm}$).

5. CONCLUSION

In conclusion, a comparative analysis of the magnetic resonance characteristics of SRRs with different formations has been performed in this work. In connection with the SRR size scaling, slit width, and substrate permittivity, it has been shown that 2C-SRRs could provide a larger shift in the magnetic resonance frequency predicted by HFSS$^{\mathrm{TM}}$. Therefore, such a 2C-SRR design could have the advantage for the tuning purpose. An approach to create a kind of tunable magnetic metamaterial has been also proposed through the 2C-SRR structure incorporating nematic LCs into the multilayered substrate. By means

of the simulated scattering parameters, it has been shown that the wide tunability ($\sim$ 1.1 GHz) of the magnetic resonance frequency in the microwave range can be easily achieved by changing the LC molecule orientation. The magnetic resonance response is of particular importance to the metamaterials and their potential applications. The 2C-SRR structure infiltrated with LCs could provide an effectual method of controlling the negative permeability and the location of the negative-index-metamaterial band.

ACKNOWLEDGMENT

The authors would like to thank the National Science Council (NSC) of Taiwan for financial support under contracts No. NSC 97-2221-E-432-001 and NSC 97-2221-E-006-079-MY3.

REFERENCES

1. Shalaev, V. M., "Optical negative-index metamaterials," *Nature Photon.*, Vol. 1, 41–48, 2007.
2. Maslovski, S., P. Ikonen, I. Kolmakov, S. Tretyakov, and M. Kaunisto, "Artificial magnetic materials based on the new magnetic particle: Metasolenoid," *Progress In Electromagnetics Research*, PIER 54, 61–81, 2005.
3. Wang, J., S. Qu, J. Zhang, H. Ma, Y. Yang, C. Gu, X. Wu, and Z. Xu, "A tunable left-handed metamaterial based on modified broadside-coupled split-ring resonators," *Progress In Electromagnetics Research Letter*, Vol. 6, 35–45, 2009.
4. Shelby, R. A., D. R. Smith, and S. Schultz, "Experimental verification of a negative index of refraction," *Science*, Vol. 292, 77–79, 2001.
5. Huangfu, J., L. Ran, H. Chen, X.-M. Zhang, K. Chen, T. M. Grzegorczyk, and J. A. Kong, "Experimental confirmation of negative refractive index of a metamaterial composed of Ω-like metallic patterns," *Appl. Phys. Lett.*, Vol. 84, No. 9, 1537–1539, 2004.
6. Chen, H. S., L. X. Ran, J. T. Huangfu, X. M. Zhang, K. S. Chen, T. M. Grzegorczyk, and J. A. Kong, "Magnetic properties of S-shaped split-ring resonators," *Progress In Electromagnetics Research*, PIER 51, 231–247, 2005.
7. Wu, W., Z. Yu, S.-Y. Wang, R. S. Williams, Y. Liu, C. Sun, X. Zhang, E. Kim, Y. R. Shen, and N. X. Fang, "Midinfrared

metamaterials fabricated by nanoimprint lithography," *Appl. Phys. Lett.*, Vol. 90, 063107, 2007.

8. Pendry, J. B., "Negative refraction makes a perfect lens," *Phys. Rev. Lett.*, Vol. 85, No. 18, 3966–3969, 2000.
9. Cai, W., U. K. Chettiar, A. V. Kildishev, and V. M. Shalaev, "Optical cloaking with metamaterials," *Nature Photon.*, Vol. 1, 224–227, 2007.
10. Wu, B., B. Li, and C. Liang, "Design of lowpass filter using a novel split-ring resonator defected ground structure," *Microwave Optical Technol. Lett.*, Vol. 49, No. 2, 288–291, 2007.
11. Alici, K. B. and E. Ozbay, "Electrically small split ring resonator antennas," *J. Appl. Phys.*, Vol. 101, 083104, 2007.
12. Lee, S.-W., Y. Kuga, and A. Ishimaru, "Quasi-static analysis of materials with small tunable stacked split ring resonators," *Progress In Electromagnetics Research*, PIER 51, 219–229, 2005.
13. Gil, I., J. Bonache, J. García-García, and F. Martín, "Tunable metamaterial transmission lines based on varactor-loaded split-ring resonators," *IEEE Trans. Microw. Theory Tech.*, Vol. 54, No. 6, 2665–2674, 2006.
14. Aydin, K. and E. Ozbay, "Capacitor-loaded split ring resonators as tunable metamaterial components," *J. Appl. Phys.*, Vol. 101, 024911, 2007.
15. Boulais, K. A., D. W. Rule, S. Simmons, F. Santiago, V. Gehman, K. Long, and A. Rayms-Keller, "Tunable split-ring resonator for metamaterials using photocapacitance of semi-insulating GaAs," *Appl. Phys. Lett.*, Vol. 93, 043518, 2008.
16. Kang, L., Q. Zhao, H. Zhao, and J. Zhou, "Ferrite-based magnetically tunable left-handed metamaterial composed of SRRs and wires," *Opt. Express*, Vol. 16, No. 22, 17269–17275, 2008.
17. Werner, D. H., D.-H. Kwon, I.-C. Khoo, A. V. Kildishev, and V. M. Shalaev, "Liquid crystal clad near-infrared metamaterials with tunable negative-zero-positive refractive indices," *Opt. Express*, Vol. 15, No. 6, 3342–3347, 2007.
18. Zhao, Q., L. Kang, B. Du, B. Li, J. Zhou, H. Tang, X. Liang, and B. Zhang, "Electrically tunable negative permeability metamaterials based on nematic liquid crystals," *Appl. Phys. Lett.*, Vol. 90, 011112, 2007.
19. Zhang, F., Q. Zhao, L. Kang, D. P. Gaillot, X. Zhao, J. Zhou, and D. Lippens, "Magnetic control of negative permeability metamaterials based on liquid crystals," *Appl. Phys. Lett.*, Vol. 92, 193104, 2008.

20. Plum, E., V. A. Fedotov, and N. I. Zheludev, "Optical activity in extrinsically chiral metamaterial," *Appl. Phys. Lett.*, Vol. 93, 191911, 2008.
21. Smith, D. R., S. Schultz, P. Markoš, and C. M. Soukoulis, "Determination of effective permittivity and permeability of metamaterials from reflection and transmission coefficients," *Phys. Rev. B*, Vol. 65, 195104, 2002.
22. Zhou, J., Th. Koschny, M. Kafesaki, E. N. Economou, J. B. Pendry, and C. M. Soukoulis, "Saturation of the magnetic response of split-ring resonators at optical frequencies," *Phys. Rev. Lett.*, Vol. 95, 223902, 2005.
23. Khoo, I. C., *Liquid Crystals*, 2nd edition, Wiley, Hoboken, 2007.
24. Khoo, I. C. and S. T. Wu, *Optics and Nonlinear Optics of Liquid Crystals*, World Scientific, Singapore, 1993.
25. Buchnev, O., E. Ouskova, Y. Reznikov, V. Reshetnyak, H. Kresse, and A. Grabar, "Enhanced dielectric response of liquid crystal ferroelectric suspension," *Mol. Cryst. Liq. Cryst.*, Vol. 422, 47–55, 2004.